

REACH OF THE CERN LHC FOR THE MINIMAL ANOMALY-MEDIATED SUSY BREAKING MODEL

Howard Baer¹, J. K. Mizukoshi² and Xerxes Tata²

¹*Department of Physics, Florida State University, Tallahassee, FL 32306 USA*

²*Department of Physics and Astronomy, University of Hawaii, Honolulu, HI 96822, USA*

(October 26, 2018)

Abstract

We examine the reach of the CERN LHC pp collider for supersymmetric models where the dominant contribution to soft SUSY breaking parameters arises from the superconformal anomaly. In the simplest viable anomaly mediated SUSY breaking (AMSB) model, tachyonic slepton squared masses are made positive by adding a universal contribution m_0^2 to all scalars. We use the event generator ISAJET to generate AMSB signal events as a function of model parameter space. Assuming an integrated luminosity of 10 fb^{-1} , the LHC can reach to values of $m_{\tilde{g}} \sim 2.3 \text{ TeV}$ for low values of m_0 , where the dilepton plus jets plus \cancel{E}_T channel offers the best reach. For large m_0 , the best signature is typically 0 or 1 isolated lepton plus jets plus \cancel{E}_T ; in this case the reach is typically diminished to values of $m_{\tilde{g}} \sim 1.3 \text{ TeV}$. The presence of terminating tracks in a subset of signal events could serve to verify the presence of a long lived lightest chargino which is generic in the minimal AMSB model.

PACS numbers: 14.80.Ly, 13.85.Qk, 11.30.Pb

The hypothesis of weak scale supersymmetry (SUSY) resolves several problems in particle physics, most notable of which is the gauge hierarchy problem. A consequence of the hypothesis is that supersymmetric matter should exist with masses typically less than ~ 1 TeV [1]. These SUSY particles are expected to be produced with large cross sections at the CERN Large Hadron Collider (LHC). Specific SUSY particle signatures, however, depend on assumptions underlying the mechanism of SUSY breaking and its mediation to the superpartners of ordinary particles.

Since dynamical SUSY breaking at the TeV scale does not appear to be possible within the framework of the Minimal Supersymmetric Standard Model (MSSM), a “hidden sector” where SUSY breaking occurs is generally assumed. SUSY breaking is then communicated to the visible sector via messenger interactions. In supergravity models, gravity acts as the messenger, and TeV level sparticle masses can arise if hidden sector SUSY breaking vevs of order $M \sim 10^{11}$ GeV can be arranged. Generically in these models, the induced soft SUSY breaking (SSB) parameters lead to problems with FCNCs and CP violating processes.

Recently, it has been noted that in supergravity models, there exist loop-suppressed contributions to soft SUSY breaking masses arising from the superconformal anomaly [2,3]. Usually, these contributions are sub-dominant compared to tree level supergravity induced mass terms. However, in the higher dimensional universe scenario of Randall and Sundrum [2], SUSY breaking can take place in a brane separated from the visible sector brane by a large distance (the sequestered sector model). In this case, tree level supergravity masses do not occur, and the anomaly mediated SUSY breaking (AMSB) mass contributions dominate.

The AMSB soft SUSY breaking gaugino masses have the special property that they are proportional to the beta functions of their corresponding gauge group:

$$M_i = \frac{\beta_i}{g_i} m_{3/2}, \quad (1)$$

where $i = 3, 2, 1$ for gauge group $SU(3)$, $SU(2)$ and $U(1)$, g_i is the corresponding gauge coupling, and $m_{3/2}$ is the gravitino mass. Similar formulae for SSB scalar squared masses and/or A parameters were worked out in [2–5]; the formulae we use are presented in [6] in the notation of the event generator program ISAJET [7] that we use for our simulation, and will not be repeated here. The characteristic features of the SSB mass terms are the following.

- Since scalar masses are proportional to their beta functions, they only depend on their respective gauge and Yukawa couplings. This guarantees universality between first and second generation scalar flavors, thus providing a solution to the SUSY flavor problem. It has been argued [2] that these models also have the potential for resolving the SUSY CP problem.
- The gaugino masses occur in the approximate ratio $M_1 : M_2 : M_3 = 2.8 : 1 : 7.1$, so that the $SU(2)$ gaugino is the lightest. This fact has profound consequences for phenomenology. The lightest neutralino \tilde{Z}_1 is dominantly a wino, and there is only a tiny mass gap between $m_{\tilde{W}_1}$ and $m_{\tilde{Z}_1}$. Including loop corrections, $m_{\tilde{W}_1} - m_{\tilde{Z}_1} \gtrsim 160$ MeV, and the decay $\tilde{W}_1^\pm \rightarrow \pi^\pm \tilde{Z}_1$ dominates, although the pion energy will be very soft. This implies that the \tilde{W}_1 will give rise to nearly invisible decay products. The

lightest chargino \widetilde{W}_1 is long lived, with values of $c\tau$ typically a few cm . It is thus possible that the \widetilde{W}_1 leaves an observable but terminating track, but whether or not this is detectable depends crucially on the detector apparatus.

- Since the Standard Model (SM) $U(1)_Y$ and $SU(2)_L$ gauge groups are not asymptotically free, negative squared masses for sleptons are predicted, leading to tachyonic states. This is viewed as the most severe shortcoming of the AMSB model, and numerous proposals have been put forth to ameliorate the situation [8]. Usually, these involve introducing new fields at intermediate scales. A simple proposal, dubbed the minimal AMSB (mAMSB) model, which is phenomenologically acceptable, is that all scalars receive an additional universal contribution m_0^2 [2,4,5], which of course, preserves the equality of masses for scalars with the same gauge quantum numbers.

Previous studies have addressed discovery of AMSB at collider experiments [9,4,5,10,11]. In [9], several new triggers for the Fermilab Tevatron $p\bar{p}$ collider experiments were suggested that exploit the highly ionizing track expected from the chargino. In [4], it is suggested that Tevatron experiments look for isolated dilepton plus missing energy events which contain in addition displaced vertices from chargino decays. In [5], it is emphasized that naturalness constraints imply light chargino masses which should generally be accessible to Tevatron searches. In Ref. [10], the AMSB scenario was examined with regard to LHC searches. Here, a detailed analysis of one case study was performed, and it was shown that many of the techniques of reconstructing sparticle masses for mSUGRA models [12] could be applied to the AMSB case. Finally, Ref. [11] discusses slepton signals at a high energy e^+e^- colliders within this framework.

An important issue in SUSY collider phenomenology is whether SUSY can be discovered or excluded over the entire range of reasonable model parameters. Although SUSY may be discovered at the Tevatron, for all distinct scenarios of SUSY breaking, there exist reasonable ranges of model parameter choices where no sparticles will be discovered [13]. However, the CERN LHC collider is frequently regarded as the definitive machine where weak scale SUSY will either be discovered or essentially disproved. The reach of the CERN LHC has been examined for the mSUGRA model for both high and low values of $\tan\beta$, and with and without R -parity violation [14,15]. The LHC reach for models with gauge-mediated SUSY breaking (GMSB) has been explored for various model lines giving rise to distinct collider signatures, and again the reach has been found to be considerable [16]. The unique sparticle mass spectrum and gaugino content of the LSP in AMSB models necessitates a distinct analysis for this class of models. In this paper, we present results showing the reach of the CERN LHC for the mAMSB model.

The mAMSB model has been presented in Ref. [4–6]. Within this framework, all sparticle masses and couplings can be calculated in terms of the parameter set:

$$m_0, m_{3/2}, \tan\beta \text{ and } \text{sign}(\mu). \quad (2)$$

The mAMSB model has recently [6] been embedded in the event generator ISAJET. In ISAJET, the weak scale gauge and Yukawa couplings are used as inputs to determine the approximate GUT scale. At M_{GUT} , the mAMSB SSB masses are calculated, and used as boundary conditions to determine their weak scale counterparts. An iterative solution is

employed in ISAJET 7.51, including 2-loop RGEs for couplings and SSB masses, and minimization of the renormalization group improved 1-loop effective potential at an optimized scale choice which effectively includes dominant 2-loop terms. Electroweak symmetry is broken radiatively (REWSB).

As far as LHC signatures go, the feature that most distinguishes the mAMSB from other frameworks (mSUGRA, GMSB) where the gaugino masses unify at M_{GUT} is that the $SU(2)$ gaugino is much lighter than the bino. Since μ is typically large, the lighter chargino (\tilde{W}_1) and neutralino (\tilde{Z}_1) are essentially wino-like with $m_{\tilde{Z}_1}$ only slightly lighter than $m_{\tilde{W}_1}$, while the second lightest neutralino (\tilde{Z}_2) is essentially a bino. This has a large impact on the cascade decay patterns of gluinos and squarks. In particular, since gluinos and \tilde{q}_L dominantly decay to $SU(2)$ -like gauginos [17], within the mAMSB framework their cascade decays do not result in hard leptons. In contrast, \tilde{q}_R now mainly decays to the hypercharge gaugino, *i.e.* via $\tilde{q}_R \rightarrow q\tilde{Z}_2$, so that \tilde{q}_R production is a potential origin of leptonic signals. This is in sharp contrast to the mSUGRA or GMSB frameworks, where these signals mainly come from \tilde{g} and \tilde{q}_L production. The jet-free trilepton signature from $\tilde{W}_1\tilde{Z}_2$ production is also expected to be small, partly because the $\tilde{W}_1\tilde{Z}_2$ cross section is small, but mainly because the \tilde{W}_1 does not decay leptonically. Thus if squarks are heavy, multilepton signals are expected to be relatively suppressed within the mAMSB framework.

We now turn to the reach of the LHC. We use the generic analysis detailed in our studies [14] of the reach within the mSUGRA framework to obtain the reach for the present case. For each point in a grid in the mAMSB parameter space, ISAJET calculates the relevant sparticle mass spectrum, and all sparticle and Higgs boson branching ratios. ISAJET then generates all SUSY $2 \rightarrow 2$ production processes, followed by cascade decays, QCD radiation in the parton shower approximation, hadronization and beam remnant evolution. The final state particles are passed to a toy detector simulation representative of LHC detectors. Calorimeter extent, cell size and energy smearing and jet finding algorithm are as given in Ref. [14], and will not be repeated here.

In each signal event, we require the presence of *i)* at least two jets, each with $E_T(jet) > E_T^c$, where E_T^c is a floating cut value designed to give some optimization of cuts throughout parameter space. We use values of $E_T^c = 100 - 500$ GeV, in steps of 100 GeV. We further require *ii)* $\cancel{E}_T > E_T^c$ and *iii)* $S_T > 0.2$, where S_T is the transverse sphericity. For multilepton events, we require each lepton $p_T(\ell) > 10$ GeV, $|\eta_\ell| < 2.5$ and visible activity in a cone of size $\Delta R = 0.3$ about the lepton direction to be less than $E_T(cone) = 5$ GeV (isolation). In addition, for events with two or more isolated leptons, the two hardest leptons in p_T should have $p_T(\ell) > 20$ GeV. In the special case of single isolated lepton events, we require $p_T(\ell) > 20$ GeV, and transverse mass $m_T(\ell, \cancel{E}_T) > 100$ GeV to suppress backgrounds from W production. The signal events are then classified according to the number of isolated leptons: 0ℓ for multijet plus missing energy events with no isolated leptons, 1ℓ for single isolated lepton events, OS for events containing two opposite sign isolated leptons, SS for events with two same-sign isolated leptons and 3ℓ for events containing three isolated leptons.

SM background rates arising from $t\bar{t}$ production, QCD multijet production, W or Z plus jets production and vector boson pair production have been calculated in Ref. [14] as a

function of E_T^c for each of the signal channels. We use the background from this paper ¹ further requiring that $E_T^c \leq 400$ GeV (300 GeV) for the OS and SS (3ℓ) channels. A signal is regarded as visible in a particular channel if, for any value of E_T^c , (i) it is 5σ above the SM background for an integrated luminosity of 10 fb^{-1} , (ii) the signal cross section is larger than 20% of the corresponding background cross section, and (iii) there should be at least 5 signal events for an integrated luminosity of 10 fb^{-1} .

Our first results are shown in Fig. 1, where we show the m_0 vs. $m_{3/2}$ parameter plane for $\tan\beta = 3$ and $\mu < 0$. The upper-left shaded region is excluded because the $\tilde{\tau}_1$ slepton becomes the LSP. The low $m_{3/2}$ shaded region is excluded by LEP2 searches for charginos in the mAMSB scenario: $m_{\tilde{W}_1} > 86$ GeV assuming a heavy sneutrino mass [18] ². Finally, in the vertically hatched region $m_h < 100$ GeV which is excluded by LEP2 searches for Higgs bosons ³. We also show contours of $m_{\tilde{g}} = 2$ TeV and $m_{\tilde{u}_R} = 2$ TeV, to orient the reader as to the parameter space. Finally, the region to the left of the dotted line is where two body decays of the neutralino \tilde{Z}_2 are allowed.

In Fig. 1, parameter space points where there is a detectable signal with 10 fb^{-1} of integrated luminosity at the LHC are denoted by triangles for the 0ℓ channel, dots for the 1ℓ channel, circles for the OS channel, squares for the SS channel, and finally, by stars for the 3ℓ channel. Points that we explored, but found no detectable signal in any of these channels, are denoted by asterisks. In the lower left, where $m_0 < 1000$ GeV and $m_{3/2} \leq 60$ TeV, the SUSY signal is visible in *all* channels considered. In this region, SUSY particle production cross sections are high, and cascade decays lead to visible signals in all channels. In the large $m_0 \sim 2000$ GeV region (where squarks are heavy) signals are observable in just the 0ℓ and 1ℓ channels as anticipated above; the reach of the LHC with just 10 fb^{-1} extends to $m_{3/2} \sim 60$ TeV, corresponding to values of $m_{\tilde{g}} \sim 1350$ GeV. In the region of parameter space with small m_0 and large $m_{3/2}$, the reach of the LHC extends up to $m_{3/2} \sim 110$ TeV, corresponding to values of $m_{\tilde{g}} \sim 2200$ GeV. In this region, the maximum reach is obtained in the OS dilepton channel. The isolated leptons arise from \tilde{g} cascade decays to $\tilde{t}_1 t$, and also from \tilde{q}_R decays to \tilde{Z}_2 which have a branching fraction close to 100%. For parameters to the left of the dotted line, \tilde{Z}_2 always decays leptonically via $\tilde{Z}_2 \rightarrow \ell\tilde{\ell}_R$ since sleptons are relatively light while squarks are heavy. (e.g. $m_{\tilde{\ell}_R} \sim 300\text{--}400$ GeV, while $m_{\tilde{q}_R} \sim 1500\text{--}2000$ GeV). The $\tilde{\ell}_R \rightarrow \ell\tilde{Z}_1$, which gives rise to a hard isolated lepton. In this region, the $\ell\bar{\ell}$ mass edge should be easily distinguished from background, and can serve as the starting point for

¹We caution the reader that these were obtained using CTEQ2L structure functions while for the signal we are using CTEQ3L structure functions.

²If the sneutrino is light the negative interference caused by the t -channel sneutrino exchange amplitude diminishes the limit to 68 GeV. The region of parameters where this might be relevant is excluded by the h mass limit.

³A preliminary combined limit of ~ 106 GeV (low $\tan\beta$) and about 88 GeV (high $\tan\beta$) was presented at SUSY2K [19] after our analysis was completed. This would enlarge the vertically shaded region, but not affect the main results of the paper which is the delineation of the region that may be explored at the LHC. We expect qualitatively similar results say for $\tan\beta = 5$.

reconstructing sparticle masses in cascade decays [20,14,12,10,21,22].

In Fig. 2, we show the LHC reach again for $\tan\beta = 3$, but for $\mu > 0$. For this sign of μ $m_h > 100$ GeV so there is no vertically hatched region. For small values of $m_0 \lesssim 300$ GeV, where the sneutrino is light, it is thus possible that the slanted hatched region is slightly too big. The reach results for the LHC are qualitatively very similar to the $\mu < 0$ case.

Finally, in Fig. 3, we show the same parameter space plane but for the large value of $\tan\beta = 35$ and $\mu > 0$. The results are expected to be independent of the sign of μ when $\tan\beta$ is large. Again the slanted hatched region is what is excluded by the chargino bound from LEP (where the same caveat as in Fig. 2 applies). The LEP limit on the h mass does not provide any further constraints. In the region of large m_0 and low $m_{3/2}$ REWSB is not obtained. We see that the reach in $m_{3/2}$ for large m_0 is similar to the low $\tan\beta$ cases, since sleptons and squarks are all very heavy in this region. Multilepton signals are obtained for $m_{3/2} = 40$ TeV and very large m_0 from cascade decays of gluinos to heavier charginos and neutralinos (which decay to real vector bosons) plus third generation quarks: for low $\tan\beta$ these decays are kinematically suppressed. However, for low values of m_0 , the reach in $m_{3/2}$ is considerably reduced compared to the low $\tan\beta$ case. Here, values of $m_{3/2} \sim 90$ TeV are accessible with 10 fb^{-1} of data, corresponding to $m_{\tilde{g}} \simeq m_{\tilde{q}} \sim 1850$ GeV. The reduction is due mainly to the large τ Yukawa coupling, which reduces the tau slepton mass compared to first and second generation slepton masses. This enhances the decay of $\tilde{Z}_2 \rightarrow \tilde{\tau}_1 \tau$ at the expense of \tilde{Z}_2 decays to $e s$ and μs . The \tilde{Z}_2 originates again mainly via cascade decay of \tilde{q}_R . The maximum reach for large $\tan\beta$ and low m_0 is attained via 1ℓ , $0S$ and 3ℓ channels. In this case, the 3ℓ events can come, for instance, from $\tilde{g}\tilde{g}$ events where $\tilde{g} \rightarrow \tilde{t}_1 t$, and where the \tilde{t}_1 has significant branching fractions into \tilde{Z}_2 , and then into leptons.

The reach that we obtain (expressed in terms of the gluino and squark masses) is similar to that in the mSUGRA framework. This is not altogether surprising since the latter reach was mainly determined by the 1ℓ channel: while our arguments suggested that the multilepton reach would be affected by the very different mass spectrum, there appeared to be no reason why the reach in the 0ℓ and 1ℓ channels should qualitatively differ. By the same token, we might expect that the overall reach would be relatively insensitive to variations of the AMSB framework. The mass difference $m_{\tilde{W}_1} - m_{\tilde{Z}_1}$ is, however, *very sensitive* to our specific model assumptions: if it is larger [10] as, for instance, in the deflected AMSB framework, then charginos would decay promptly, and its decay products might be visible, making the signal more “mSUGRA-like”.

In conclusion, the CERN LHC pp collider should be able to discover supersymmetry with just 10 fb^{-1} of integrated luminosity, over most of the mAMSB parameter space where $m_{\tilde{q}} < 2$ TeV, or where $m_{\tilde{g}} < 1300$ GeV regardless of $m_{\tilde{q}}$. Moreover, these signals should be observable via canonical strategies [14,15] advocated for SUSY searches in the mSUGRA framework. As in this case, over a large region of parameter space, there should be observable signals in several channels. Once a signal is found, then signal events may be scrutinized for evidence of tracks from long lived charginos, which occasionally penetrate into tracking chambers. These tracks should either terminate, or result in a kink from the slow pion daughter of the \tilde{W}_1 . Observability, if at all possible, will require large event rates since $c\tau$ for the decaying chargino is less than 5 cm and we would be relying on charginos that live for several lifetimes for this purpose: this feature cannot, therefore, be used to extend the reach. The rate will be sensitive to detector characteristics and any instrumental backgrounds. The

terminating tracks could serve to distinguish the mAMSB model from other scenarios.

ACKNOWLEDGMENTS

This research was supported in part by the U. S. Department of Energy under contract number DE-FG02-97ER41022 and DE-FG-03-94ER40833.

REFERENCES

- [1] For reviews of weak scale supersymmetry phenomenology, see M. Dine, hep-ph/9612389 (1996); M. Drees, hep-ph/9611409 (1996); S. P. Martin, hep-ph/9709356 (1997); X. Tata, hep-ph/9706307 (1997); S. Dawson, hep-ph/9709356 (1997).
- [2] L. Randall and R. Sundrum, Nucl.Phys. **B557**, 79 (1999).
- [3] G. Giudice, M. Luty, H. Murayama and R. Rattazzi, JHEP **9812**, 027 (1998).
- [4] T. Gherghetta, G. Giudice and J. D. Wells, Nucl. Phys. **B559**, 27 (1999).
- [5] J. L. Feng and T. Moroi, Phys. Rev. D**61**, 095004 (2000).
- [6] H. Baer, M. Diaz, P. Quintana and X. Tata, JHEP **0004**, 016 (2000).
- [7] F. Paige, S. Protopopescu, H. Baer and X. Tata, hep-ph/0001086 (2000).
- [8] A. Pomarol and R. Rattazzi, JHEP **05**, 013 (1999); R. Rattazzi, A. Strumia and J. D. Wells, hep-ph/9912390 (1999); Z. Chacko, M. Luty, I. Maksymyk and E. Ponton, JHEP **04**, 001 (2000); E. Katz, Y. Shadmi and Y. Shirman, JHEP **08**, 015 (1999); I. Jack and D. R. T. Jones, Phys. Lett. **B482**, 167 (2000); B. C. Allanach and A. Dedes, JHEP **06**, 017 (2000).
- [9] J. L. Feng, T. Moroi, L. Randall, M. Strassler and S. Su, Phys. Rev. Lett. **83**, 1731 (1999).
- [10] F. Paige and J. D. Wells, hep-ph/0001249 (2000).
- [11] D. K. Ghosh, P. Roy and S. Roy, hep-ph/0004127 (2000).
- [12] I. Hinchliffe, F. Paige, M. Shapiro, J. Soderqvist and W. Yao, Phys. Rev. D**55**, 5520 (1997).
- [13] V. Barger and C. Kao, Phys. Rev. D**60**, 115015 (1999); H. Baer, M. Drees, F. Paige, P. Quintana and X. Tata, Phys. Rev. D**61**, 095007 (2000); K. Matchev and D. Pierce, Phys. Lett. **B467**, 225 (1999); for a review, see S. Abel *et al.*, hep-ph/0003154 (2000).
- [14] H. Baer, C. H. Chen, F. Paige and X. Tata, Phys. Rev. D**52**, 2746 (1995) and Phys. Rev. D**53**, 6241 (1996); H. Baer, C. H. Chen, M. Drees, F. Paige and X. Tata, Phys. Rev. D**59**, 055014 (1999); H. Baer, C. H. Chen and X. Tata, Phys. Rev. D**55**, 1466 (1997).
- [15] S. Abdullin *et al.*, (CMS Collaboration), hep-ph/9806366 (1998); ATLAS Technical Design Report, V 2, CERN/LHCC/99-15 (1999).
- [16] H. Baer, P. Mercadante, F. Paige, X. Tata and Y. Wang, Phys. Lett. **B435**, 109 (1998); H. Baer, P. Mercadante, X. Tata and Y. Wang, hep-ph/0004001 (2000).
- [17] H. Baer, V. Barger, D. Karatas and X. Tata, Phys. Rev. **D36**, 96 (1987).
- [18] G. Grenier, talk given at SUSY2K meeting, CERN, Geneva, June, 2000.
- [19] See talk by T. Junk, SUSY2K meeting, CERN, Geneva, June, 2000.
- [20] H. Baer, C. H. Chen, F. Paige and X. Tata, Phys. Rev. D**50**, 4508 (1994);
- [21] D. Denegri, W. Majerotto and L. Rurua, Phys. Rev. D**58**, 095010 (1998).
- [22] M. M. Nojiri and Y. Yamada, Phys. Rev. D**60**, 015006 (1999).

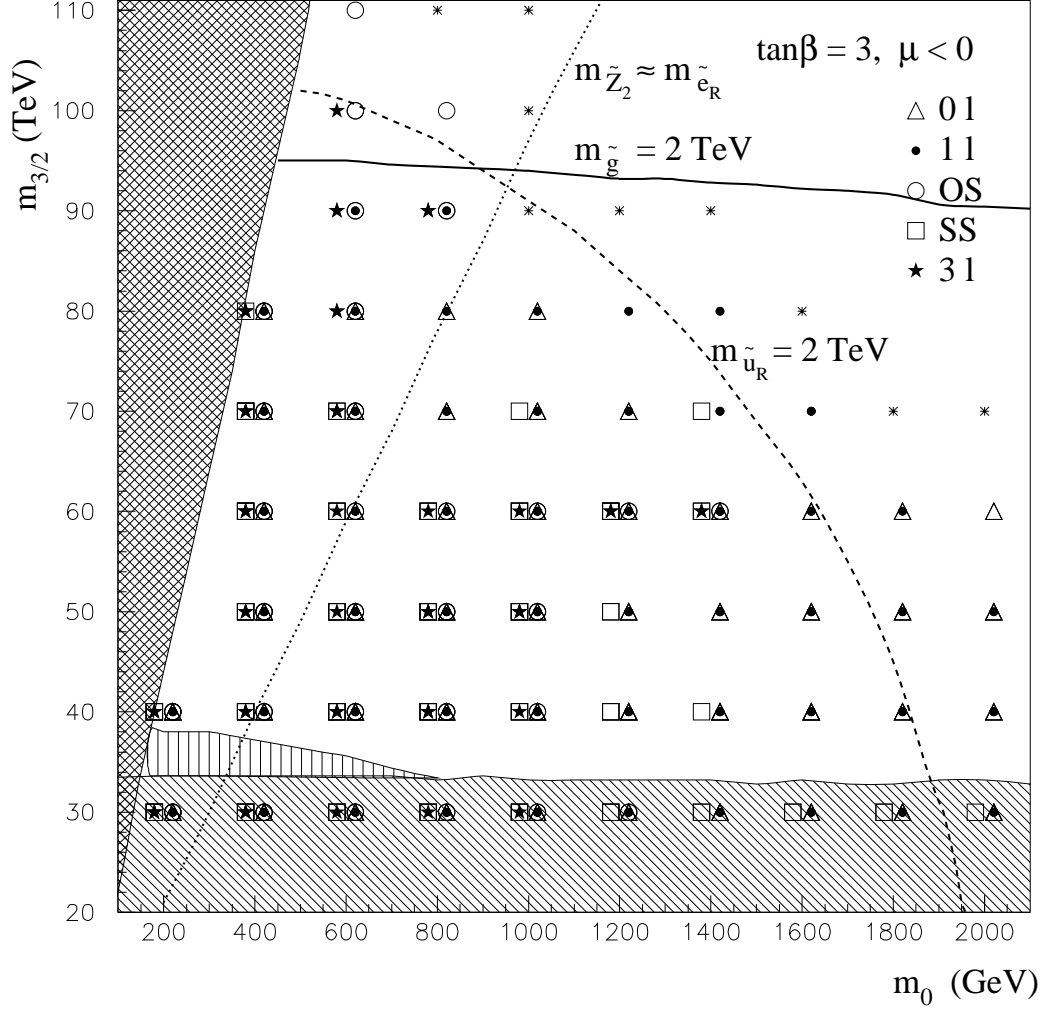


FIG. 1. A plot of the m_0 vs. $m_{3/2}$ plane for $\tan\beta = 3$ and $\mu < 0$. The shaded regions are excluded by theoretical and experimental constraints as discussed in the text. Each point in the parameter space scanned is denoted by one or more symbols corresponding to whether the SUSY signal for the point is detectable in any of the 0ℓ , 1ℓ , OS , SS or 3ℓ channels at the CERN LHC, assuming 10 fb^{-1} of integrated luminosity. Our criteria for detectability are detailed in the text.

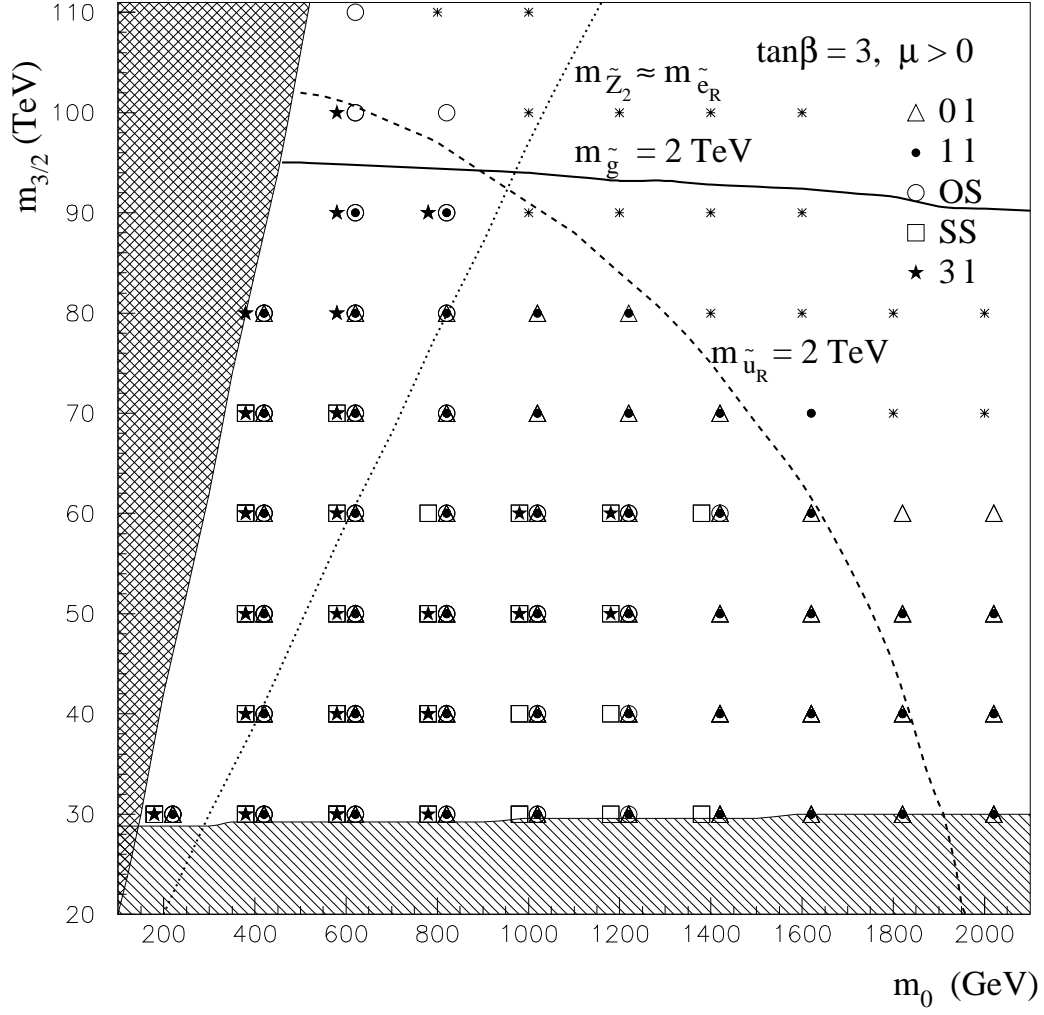


FIG. 2. Same as Fig. 1, except we take $\mu > 0$.

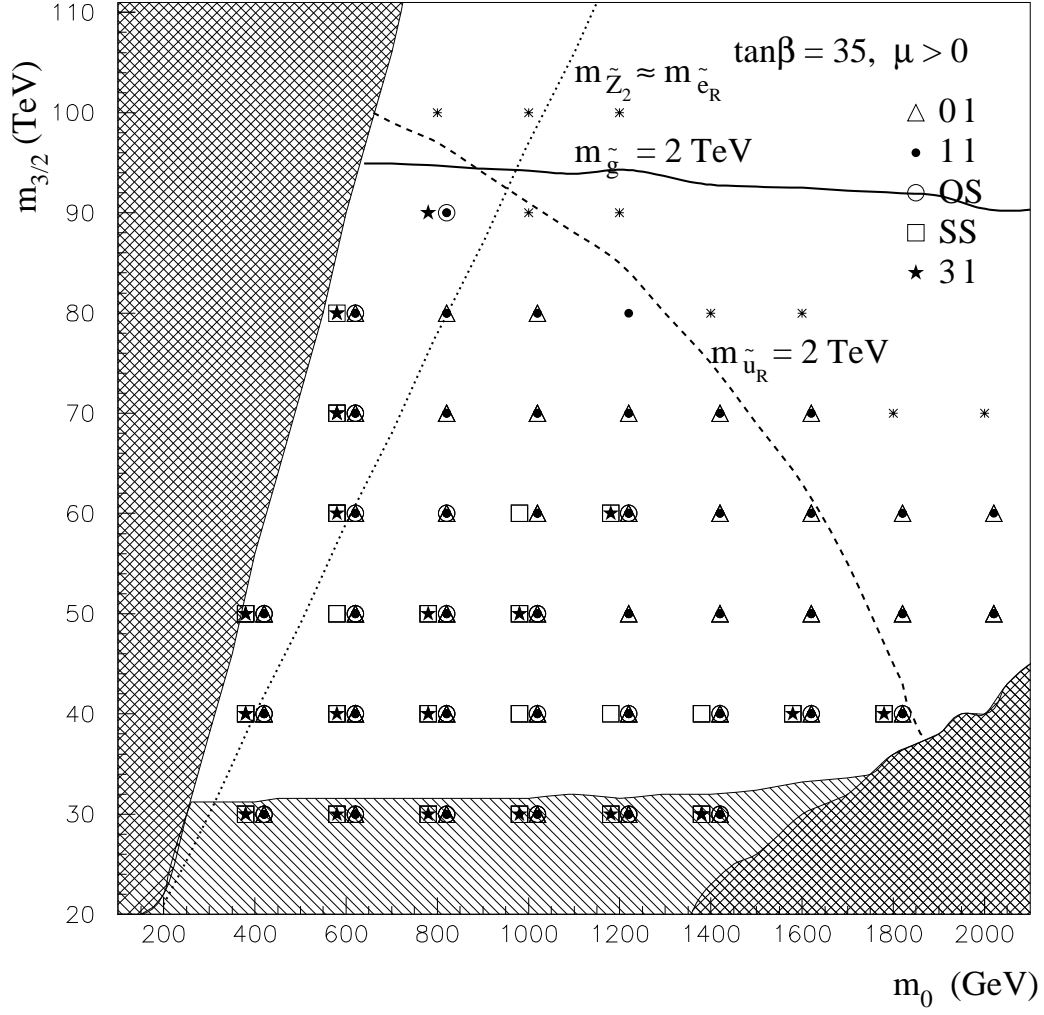


FIG. 3. Same as Fig. 1, except we take $\tan\beta = 35$, and $\mu > 0$.